AD-A187 482 THE ANALYSIS OF DEFORMATIONS AND STRAINS IN COMPOSITES 1/1
BY MOIRE INTERFEROMETRY(U) VIRGINIA POLYTECHNIC INST
AND STATE UNIV BLACKSBURG DEPT OF E D POST JUL 87
UNCLASSIFIED N00014-86-K-0255 F/G 11/4 NL

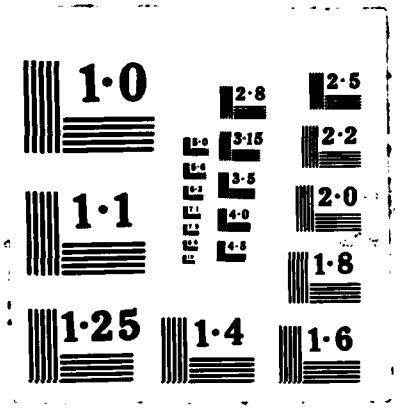
1·0
1·1
1·25
1·4
1·6
1·8
2·0
2·2
2·5
2·8
3·15
3·5
4·0
4·5

Contract N00014-86-K-0255

THE ANALYSIS OF DEFORMATIONS AND STRAINS IN COMPOSITES BY MOIRE INTERFEROMETRY

Daniel Post
Engineering Science and Mechanics Department
Virginia Polytechnic Institute and State University
Blacksburg, Virginia 24061, USA

ABSTRACT

Local deformation fields are exhibited for several composite members. Cases of severe shear strain gradients and local anomalies of material behavior are emphasized. Examples illustrated are from short beam tests, strain concentration analyses, multiply panel tests and slotted metal-matrix tensile specimen tests. The experimental method, moire interferometry, yielded contour maps of in-plane displacement fields with subwavelength sensitivity, high fringe contrast and high spatial resolution.

INTRODUCTION

The deformations of composite members are replete with cases of severe strain gradients. Also, locally nonuniform or anomalous material behavior is frequently encountered. These qualities cannot be detected or measured by conventional tools like strain gages or extensometers. A method with high spatial resolution and high sensitivity is needed and moire interferometry provides these qualities.

This paper surveys some of the work conducted on composite members at the author's laboratory. The examples shown here emphasize a diversity of local effects that must be studied to understand the behavior of composites. A common link is the strong influence of shear on deformation of composites, and the concomitant influence of matrix thickness on shear strain magnitudes.

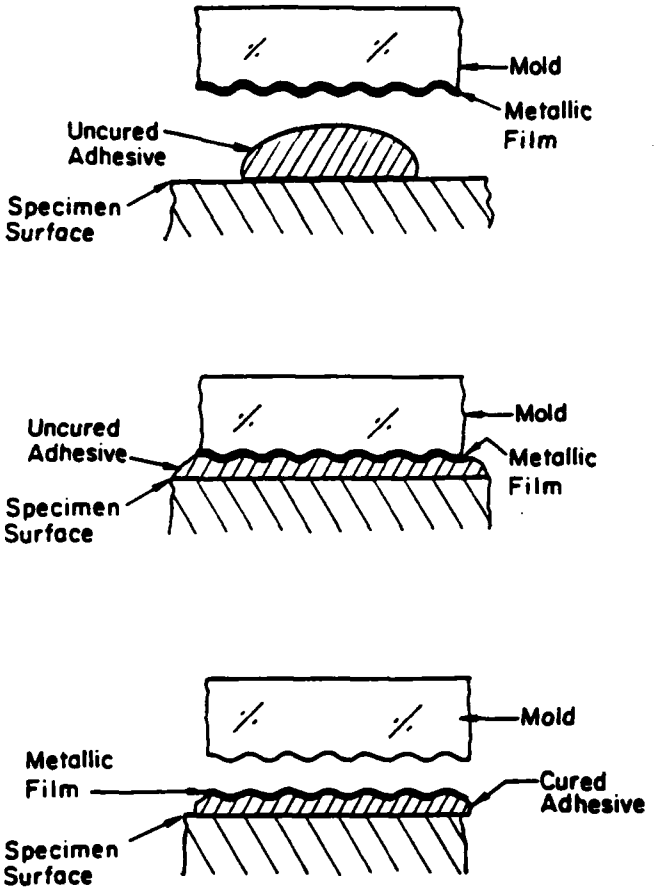

Fig. 1.
(a) Replication technique to form a high-frequency, high-reflectance, crossed-line grating on the specimen.
(b) Four-beam optical arrangement for moire interferometry.

EXPERIMENTAL METHOD

Deformations were determined by moire interferometry. This is an optical method that produces whole-field contour maps of in-plane displacement components, U and V. Sensitivity was in the subwavelength range, 0.417 μm (16.4 μin.) per fringe order. In addition to high sensitivity, the method is characterized by high contrast interference fringes and high spatial resolution. While it is similar in many ways to classical and holographic interferometry, which are techniques primarily useful for out-of-plane displacement measurements, W, moire interferometry provides the important in-plane displacements -- the displacements related directly to strains.

Detailed descriptions of moire interferometry appear in Refs. 1 and 2. Briefly, a high frequency crossed-line diffraction grating is replicated on the specimen surface using a special mold, as illustrated in Fig. 1a. The result is a thin -- 0.025 mm (0.001 in.) -- reflective phase grating firmly adhered to the specimen, which deforms together with the specimen surface. The initial frequency of the specimen grating, before loads are applied, is f/2.

The specimen grating is observed in an optical arrangement illustrated schematically in Fig. 1b. Two beams of coherent light from C' and D' intersect at an angle of 2α in the horizontal plane and form a virtual reference grating with its grating lines perpendicular to the x direction. Beams from A' and B' intersect at 2α in a vertical plane and form a virtual reference grating with lines perpendicular to the y direction. The frequency of each virtual reference grating is $f = (2\sin\alpha)/\lambda$, where λ is the wavelength of the light. Each reference grating interacts with the similarly oriented lines of the specimen grating to form the interference patterns recorded in the camera. The patterns are contour maps of displacements governed by the relationships

$$U = \frac{1}{f} N_x \qquad V = \frac{1}{f} N_y \tag{1}$$

where U and V are in-plane x and y components of displacement at any point; N_x and N_y are the fringe orders at that point in the corresponding fringe patterns, i.e., the patterns formed using grating lines perpendicular to the x and y directions, respectively.

Strains can be calculated from the displacement fields by the (small strain) relations

$$\varepsilon_x = \frac{\partial U}{\partial x} = \frac{1}{f}\left(\frac{\partial N_x}{\partial x}\right) \qquad \varepsilon_y = \frac{\partial V}{\partial y} = \frac{1}{f}\left(\frac{\partial N_y}{\partial y}\right) \tag{2}$$

$$\gamma_{xy} = \frac{\partial U}{\partial y} + \frac{\partial V}{\partial x} = \frac{1}{f}\left(\frac{\partial N_x}{\partial y} + \frac{\partial N_y}{\partial x}\right) \tag{3}$$

where ε_x and ε_y are normal strains in the x and y directions, respectively, and γ_{xy} is shear strain. In this work, f was 2400 lines/mm (60,960 ℓ/in). Sensitivity, or displacement per fringe order, is the reciprocal of f.

SHORT BEAMS

Figure 2a illustrates deformations in a 48 ply quasi-isotropic graphite-epoxy beam under 3-point loading. The specimen grating was applied to the edge of the beam, covering all 48 plies. The pattern is the N_x or U displacement field for the portion indicated by the dashed box. It exhibits a pronounced cyclic distribution of $\partial N_x/\partial y$ across any vertical section. Shear strains were calculated along line B-B from this, plus information from the companion N_y pattern, with the result shown in the graph. The dramatic undulations of shear strains are attributed to two effects. Near the center of the beam height, where shear stresses are large, they are associated with the cyclically varying shear compliance of the successive plies. Near the top and bottom, where the normal stresses are large, they are associated with free-edge effects of multi-angle laminates.[3]

Figure 2b illustrates a 48 ply quasi-isotropic graphite-PEEK beam under 5-point loading. Here, the N_y field is transformed by a carrier pattern such that the slope of any fringe at section AA' is proportional to $\partial N_x/\partial y$. The shear strains along AA' reveal sharp peaks or spikes on an otherwise cyclic distribution. These spikes are attributed to resin-rich zones between plies, zones of high shear compliance that allow large shear displacements under shear loading.[4]

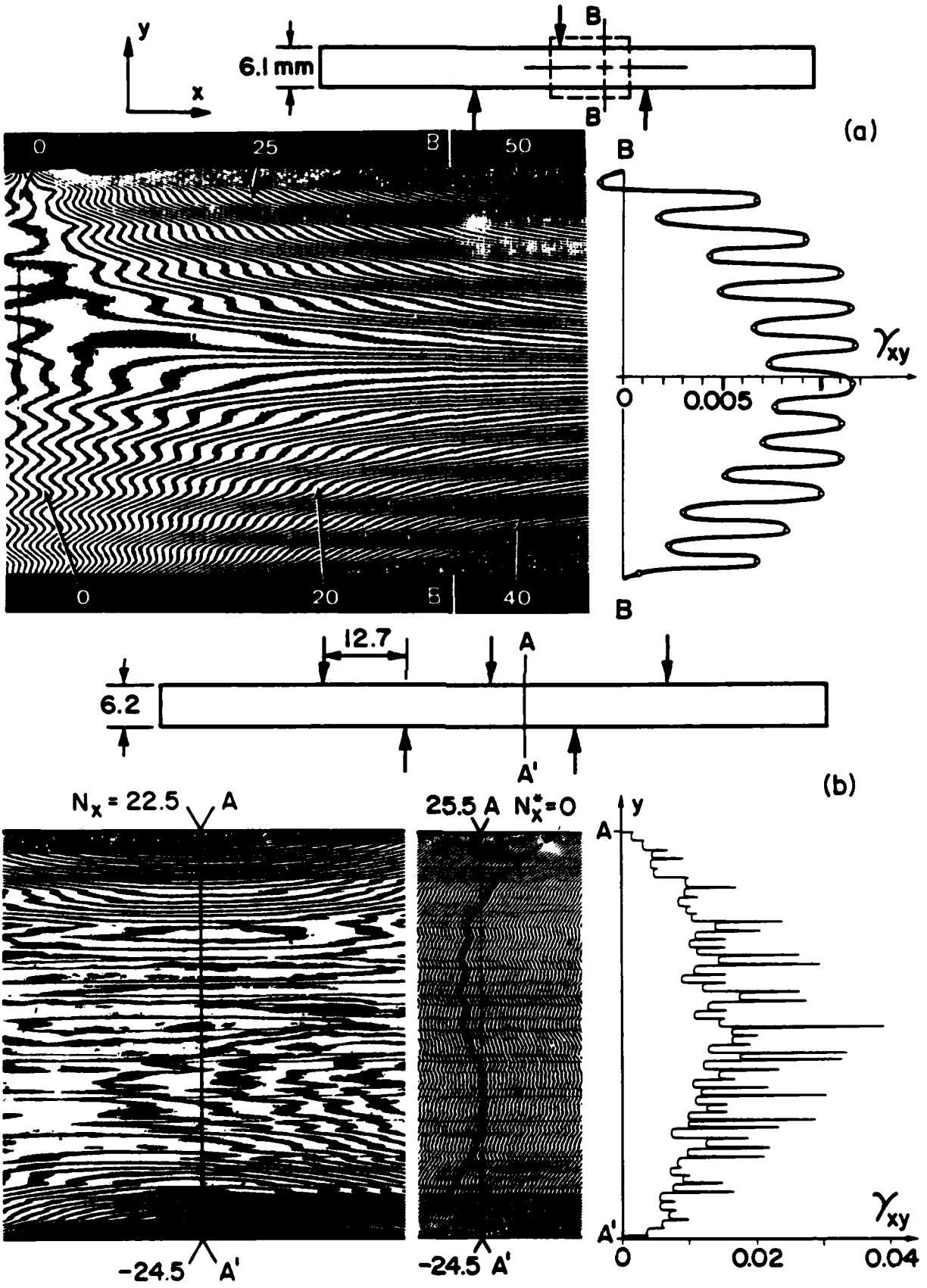

Fig. 2. N_x or U field for short-beam specimens, and shear strain on a cross-section. (a) Graphite-epoxy. (b) Graphite-PEEK; pattern in center shows N_x with carrier fringes.

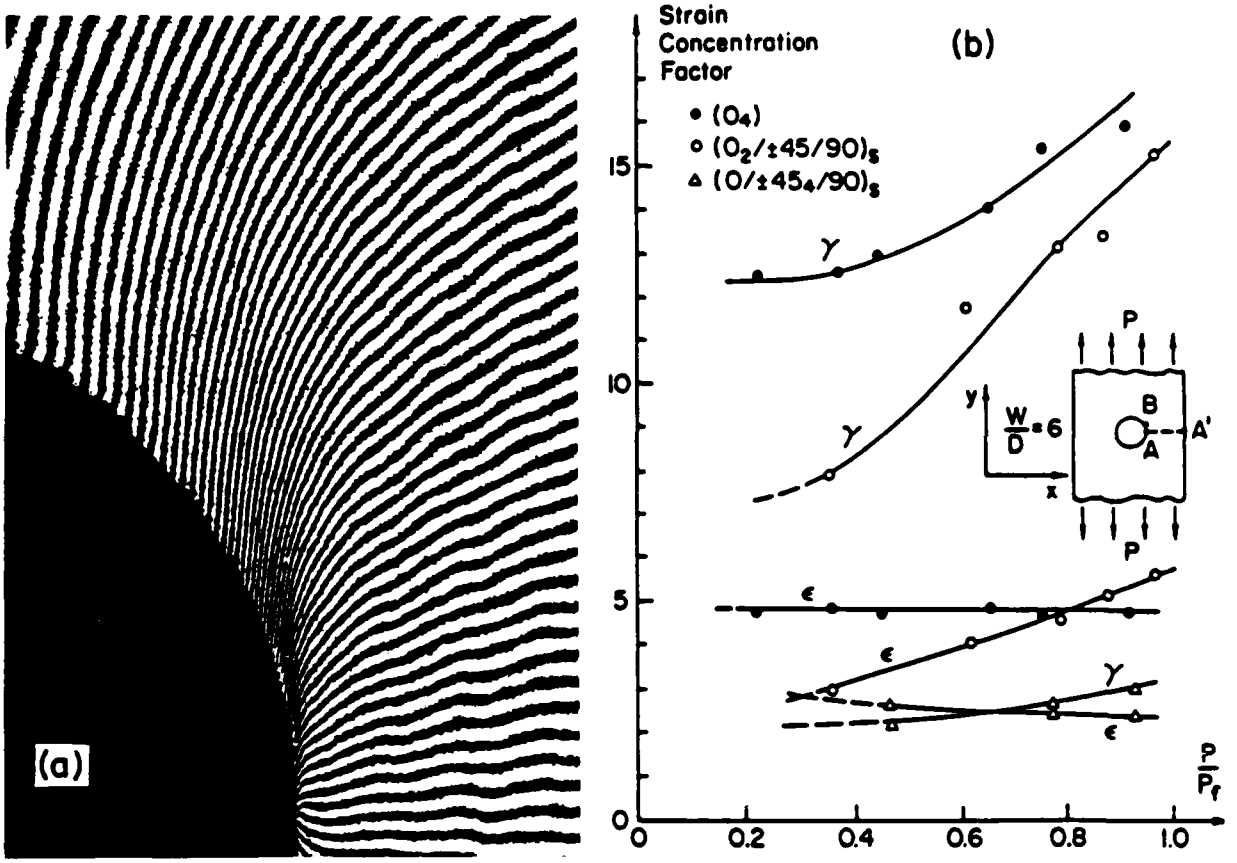

Fig. 3. (a) N_y or V field in a multi-ply graphite-epoxy tensile specimen with a central hole; hole diameter is 6.3 mm (0.25 in.). (b) Influence of load level on normal (ε) and shear (γ) strain concentration factors; P_f is failure load.

STRAIN CONCENTRATIONS

Strain concentrations in composites can occur in regions of extremely high gradients, as illustrated in Fig. 3. The specimen was a graphite-epoxy tensile member with a central hole. The hole diameter was 6.3 mm (0.250 in.), the specimen width was 6 times greater, and the stacking sequence was $(0_2/\pm45/90)_s$. Only a small portion of the fringe pattern is shown, greatly enlarged. Patterns of U and V displacements were recorded at several load levels, P, up to the failure load, P_f, where failure was defined as the appearance of the first visible crack in the specimen.

Normal strains and shear strains were determined at points A and B, respectively, from these patterns. These corresponded to points of maximum displacement gradients and correspondingly, points of maximum strains. Strain concentration factors were defined as the maximum strains normalized by the average strain ε_y on ligament A-A'. The normal and shear strain concentration factors are plotted in Fig. 3b against load for this specimen and for two other specimens with stacking sequences as shown.[5]

Fig. 4.
Nonuniform or anomalous part of the transverse field N_x in a graphite-epoxy panel. Stacking sequence $[0_2/\pm60/0_2/\pm60]_s$. Uniform specimen width of 25 mm (1 in.).

MATERIAL ANOMALIES

The method of moire interferometry allows an adjustment of the reference grating that can be used to subtract off any uniform strain field.[1,6] Figure 4 depicts the nonuniform part of the N_x (transverse displacement) field in a tensile specimen of uniform cross-section; fringes that would otherwise be caused by the uniform part of the ε_x field were cancelled. The corresponding average axial strain was ε_y = 9000 μm/m. The tensile coupon was cut from a (commercially produced) graphite-epoxy panel of ply sequence $[0_2/\pm60/0_2/\pm60]_s$.

The strongest anomalies occur in bands at ±60 deg and they result, presumably, from imperfections in the ±60 deg plies -- the third and fourth plies from the surface. In the region of largest fringe gradients, $\partial U/\partial x$ = 1500 μm/m and $\partial V/\partial x$ = 3000 μm/m. The strains at corresponding locations in the interior must have been larger, being attenuated as they were transmitted to the surface. The anomalous strains were rather large.

METAL-MATRIX

Moire interferometry cannot cope with the general micromechanics problem today, but it can be used effectively when the microstructure is relatively coarse. The metal-matrix composite problem of Fig. 5 is an example. The specimen was a tensile coupon with a central slot. It was made of boron fibers in a ductile aluminum matrix, with a 6 ply stacking sequence of $[0/\pm45]_s$. The slot width was 5.5 mm and the fiber diameter was 0.14 mm.

The most severe fringe gradients appear in narrow zones of matrix material, lying adjacent to the first discontinuous fiber at each end of the slot. These are plastic slip zones, where shear strains extend well into the plastic range of the aluminum matrix. Figure 5b shows the variation of the maximum shear strain with load level.

The zig-zag fringes are real deformation effects, not optical noise of the experiments. These fringes have smaller slopes where they lie over the stiff fibers and larger slopes over the more compliant matrix material. They signify low values of $\partial V/\partial x$ in the fibers and higher values in the matrix, and they indicate the higher shear strains in the matrix.[7,8]

The specimen of Fig. 6 had the same configuration, except the stacking sequence was $[\pm45/0_2]_s$; the outer fibers had 45 deg orientation. A special optical technique (utilizing beams from A' and D' in Fig. 1b, or B' and C') was used to obtain the ±45° displacement fields,[9] displacements parallel and perpendicular to the fibers of the outer ply. The far-field strain for this set of patterns was nearly the same as that for Fig. 5. The patterns are redundant, since any two orthogonal fields fully define the in-plane deformation. Nevertheless, they offer an immense advantage for visual interpretation and ease of data reduction.

The great similarity between Figs. 5 and 6a indicates that the global deformation is essentially the same in the 0 deg and 45 deg plies. The local deformations in plies, however, are rather different. The plastic slip zones of the 0 deg plies do not occur at corresponding locations in 45 deg plies. The zig-zag fringes showing local fiber/matrix movements are different in Figs. 5 and 6. Figure 6d also shows numerous lines of slip between neighboring 45 deg fibers, while 6c shows continuity of the orthogonal displacements in the same locations. This means that the

relative motion is strictly along the fiber direction, and that shear deformations between certain fibers substantially exceed those of neighboring fiber pairs. This anomalous distribution of shear strains might be attributed to local variations of thickness of matrix material between fibers in the ply, and also local variations of matrix thickness between adjacent plies. Summarizing, deformation of the various plies exhibit marked local differences, but great global similarity.

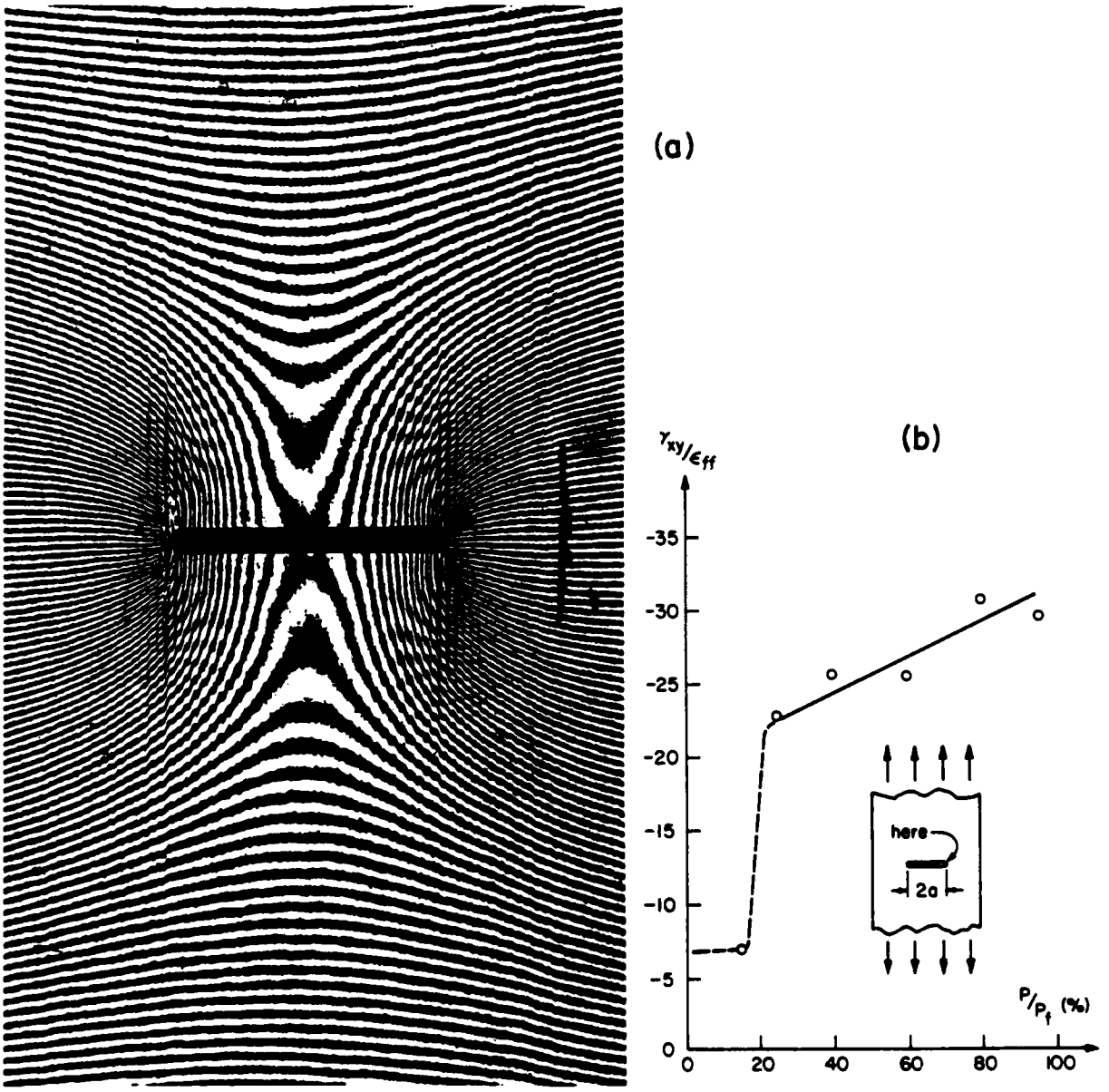

Fig. 5. (a) N_y or V field in a boron-aluminum tensile specimen with a central slot. Stacking sequence $[0/\pm45]_s$. Slot length 5.5 mm (0.22 in.). P/P_f = 60%. (b) Shear-strain concentration factor at point of maximum shear strain; ϵ_{ff} is the far-field normal strain.

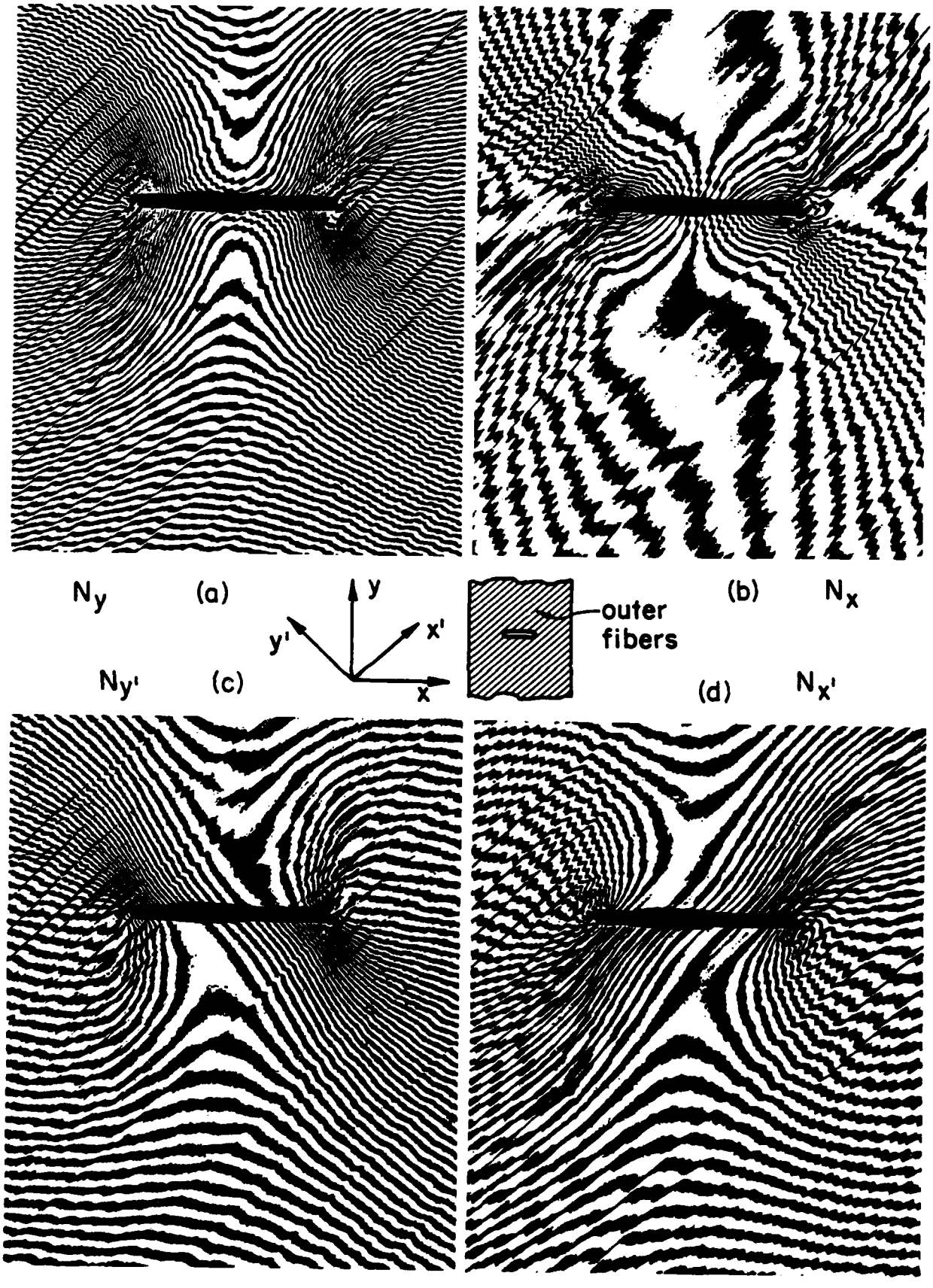

Fig. 6. Displacement fields in a similar specimen, but with stacking sequence $[\pm 45/0_2]_s$. Sensitivity for ±45 deg patterns is $\sqrt{2}/f$ or 0.589 μm per fringe order; for others, sensitivity is 1/f or 0.417 μm/fringe.

ACKNOWLEDGEMENTS

This paper was compiled under the sponsorship of the Office of Naval Research under Project No. N00014-86-K-0255. Applications shown in the figures were sponsored by NASA Langley Research Center (Figs. 2, 5 and 6), Bell Helicopter Textron (Fig. 3) and National Science Foundation (Fig. 4). This sponsorship and permission to use the figures is gratefully acknowledged.

REFERENCES

1. D. Post, "Moire Interferometry," Chap. 7, Handbook of Experimental Mechanics, A. S. Kobayashi, Editor, Prentice-Hall, Englewood Cliffs, NJ (1986).

2. D. Post, "Moire Interferometry at VPI & SU," Experimental Mechanics, 23(2), pp. 203-210 (June 1983).

3. D. Post, R. Czarnek, D. Joh, and J. Wood, "Deformation Measurements of Composite Multi-Span Beam Shear Specimens by Moire Interferometry," NASA Contractor Report 3844 (Nov. 1984).

4. D. Post, R. Czarnek and D. Joh, "Shear Strains in a Graphite-Peek Beam by Moire Interferometry with Carrier Fringes," Proceedings of the 1986 SEM Fall Conference on Experimental Mechanics, Keystone, CO (Nov. 1986). Also Experimental Mechanics, to be published.

5. D. Post, R. Czarnek and Y. Guo, "Tensile and Shear Strain Concentration Factors in Composite Tensile Members with Central Holes," Proceedings of the Third Annual Review, Virginia Tech Center for Composite Materials & Structures (April 1986).

6. R. Czarnek, D. Post and Y. Guo, "Nonuniformities in Composite Panels by Moire Interferometry", Proceedings of the 1986 SEM Spring Conference on Experimental Mechanics, New Orleans, LA (June 1986).

7. D. Post, R. Czarnek, D. Joh, J. Jo and Y. Guo, "Elastic-Plastic Deformation of a Metal-Matrix Composite Coupon with a Central Slot," NASA Contractor Report No. 178013 (Nov. 1985).

8. D. Post, R. Czarnek, D. Joh, J. Jo and Y. Guo, "Deformation of a Metal-Matrix Tensile Coupon with a Central Slot: an Experimental Study," Jl. of Composites Technology and Research, Vol. 9, No. 1 (Spring 1987).

9. R. Czarnek and D. Post, "Moire Interferometry with ± 45-deg Gratings," Experimental Mechanics, 24(1), 68-74 (March 1984).

END

Feb.

1988

DTIC